ARCHIVES OF ELECTRICAL ENGINEERING VOL. 67(1), pp. 37–49 (2018)

DOI 10.24425/118990

Conception of the throttle-return valve for the magnetorheological fluid

ZBIGNIEW PILCH, JAROSŁAW DOMIN

Silesian University of Technology
Faculty of Electrical Engineering, Mechatronic Department
44-100 Gliwice, Poland
e-mail: zbigniew.pilch@polsl.pl, jaroslaw.domin@polsl.pl

(Received: 30.09.2016, revised: 19.02.2017)

Abstract: The paper presents the concept of the throttle-return valve dedicated for magnetorheological fluid. Basic properties of the magnetorheological fluid, valve conception and field calculations were presented.

Key words: magnetorheological fluid, throttle valve, return valve, throttle-return valve, FEMM

1. Introduction

Modern SMART materials (with special properties) give the possibility of designing and constructing devices whose functionality can be significantly higher than traditional solutions (due to these special properties). Liquids of varying viscosity (magnetorheological, electrorheological) belong to one of the seven groups of smart materials.

The real development of manufacturing technology of magnetic fluids and their use in technical applications occurred in the 90s of the twentieth century, when the US company LORD Corporation introduced magnetorheological fluid for commercial sale. The carrier material was: mineral oil (e.g. 132LDMRF), silicon (e.g. MRF336AG) and water (241ESMRF) [7]. Nowadays, liquid with hydrocarbons as carrier materials are used (MRF122EG, MRF132-2DG, or MRF140CG). A kinematic viscosity η (without magnetic field) for liquids currently produced is several (over a dozen) times smaller than for the older generation liquids. Simultaneously the value of shear stress, which can be obtained for currently available liquids, is about 3 times higher compared to the previous generation of liquids [6].

Prevailing solutions and applications assume that the magnetorheological fluids can work in three basic modes [6]:

– liquid works in flow mode (the so-called **valve mode**) – liquid flows between the fixed walls in the perpendicular directions to the magnetic flux. The mode valve as a concept is illustrated in Fig. 1.

– liquid works in clutch mode – one of the walls limiting the volume of liquid is stationary or walls velocities are different and the direction of magnetic flux is perpendicular to the wall surface,
– liquid works in compressive/tensile mode – elements limiting the area with the liquids move apart and the direction of magnetic flux coincides with the pole piece direction.

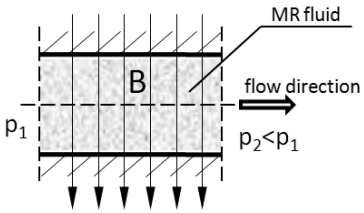

Fig. 1. The liquid flow for valve mode

The described work modes of magnetorheological fluid are used in many different constructions. One of the most interesting groups is a group of valves with flow direction control. In the paper [3] a solution for a 4/3 valve which allows one to control the direction of movement of the 2-way actuator was proposed. The proposed solution allows one to combine a directional control operating mode with control of an actuator velocity. In [2] the construction of a throttle valve with an additional non-magnetic duct was contemplated. The purpose of this modification was to change the flow velocity versus the pressure difference curve $v = f(\Delta p)$.

In the next paper [4] an analysis of the valve with flow control of magnetorheological fluid with used field method MES was presented. In [15] the authors proposed an interesting solution of the shock absorber with a screw valve controlling the fluid flow between the chambers of the actuator. Paper [10] presents the concept of the throttle valve/non-return with the hybrid excitation field (permanent magnet and coil).

In [9] a solution for the construction of a pressure valve was proposed. Maintaining the required pressure in the system is carried out by changing the current value of the coil valve.

2. The basic properties of the MR fluid

MR fluid properties depend mainly on the percentage (by weight) of solids content which, for MRF140CG reaches almost 85.5%. Shear stress τ versus flux density B curve is shown in Fig. 2.

Data points known from the literature [12] are marked, and the approximating function takes the form:

$$\tau_0(B) = \left(-49.14 \cdot B^3 + 62.4 \cdot B^2 + 45.47 \cdot B + 0.1959\right) \cdot 10^3 \ \text{(Pa)}. \tag{1}$$

Other parameters of the MRF140 CG liquid [12]: density 3.54–3.74 g/cm^3, working temperature -40°C to 130°C, dynamic viscosity 0.28 ± 0.07 Pa·s, ignition temperature > 150°C.

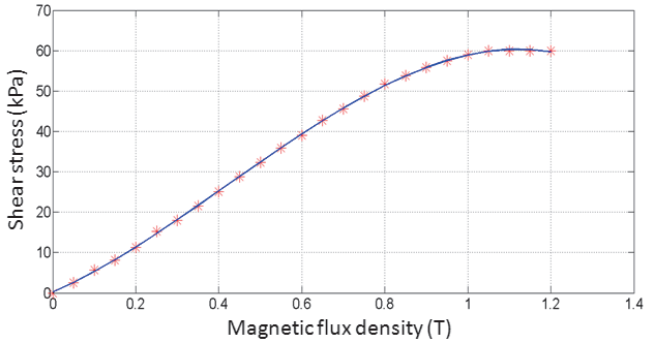

Fig. 2. Shear stress τ versus flux density B curve for MRF140CG

3. The concept of throttle-return valve

The throttle-return valves are commonly used in fluid drives. They serve to limit the displacement velocity of the actuator in one direction. When the fluid flow is forced in the opposite direction, the flow is free – the actuator is moving at maximum velocity.

The hydraulic diagram of this type of valve with determination of flow rates for the two directions of flow movement is presented in Fig. 3.

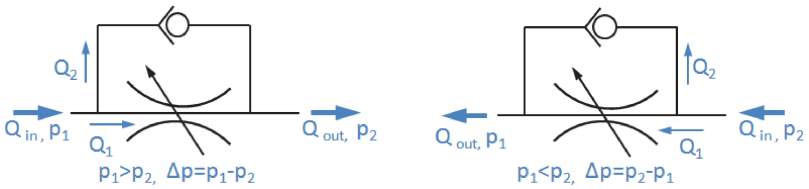

Fig. 3. Hydraulic diagram of throttle-return valves

For cases indicated in Fig. 3:

a) $p_1 > p_2$, $Q_{\text{aut}} = Q_1 + Q_2$, where $Q_2 \gg Q_1$ (return valve oriented in the flow direction),

b) $p_1 > p_2$, $Q_{\text{aut}} = Q_1$, and $Q_2 = 0$ (return valve oriented in blocking direction).

In Fig. 4 presented the conception of the throttle-return valve dedicated for flow control of the magnetorheological fluid.

The idea of the valve is based on the separation of the incoming liquid flux Q_{in} into two fluxes Q_1 and Q_2. The flux Q_1 flows through the part of the valve, which is responsible for the controlled flow, depending on the power supply coil 1, whereas flux Q_2 assumes the value 0 for the coil current $i = i_{\max}$ (closing of the valve), and the maximum value for $i = 0$ (opening of the valve).

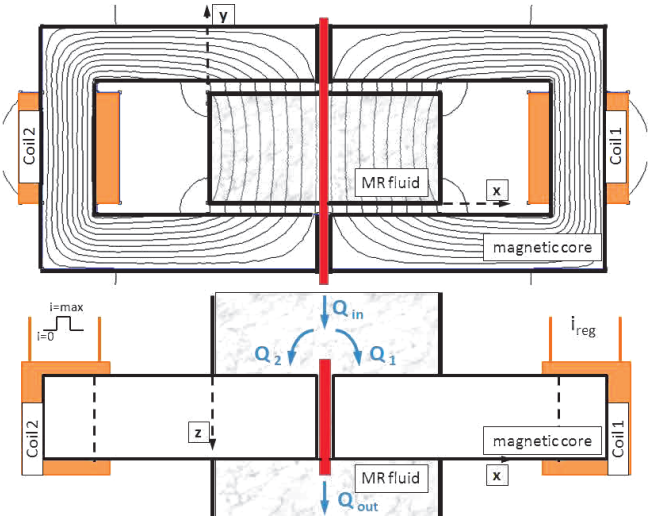

Fig. 4. Design idea of the throttle-return valve dedicated for the magnetorheological fluid

Shear stress change for magnetorheological fluid is described (in accordance with the model Bingham) by:

$$\tau = \operatorname{sgn}\left(\frac{\mathrm{d}\gamma}{\mathrm{d}t}\right)\tau_0(B) + \mu\frac{\mathrm{d}\gamma}{\mathrm{d}t}, \tag{2}$$

where: τ is the shear stress, $\tau_0(B)$ is the shear stress limit value as a function of magnetic flux density B, μ is the dynamic viscosity of the liquid, γ is the liquid deformation.

4. Field method calculation for throttle-return valve

The curve presented in Fig. 2 shows that the value of magnetic flux density above 1 T will not increase the value of shear stress. Therefore, the field excitation system should be designed so that the direction of magnetic flux is perpendicular to the direction of fluid flow and controllable in the range of magnetic flux density 0 to 1.1 T.

Selection of the electro-magnetic circuit parameters was realized according to an algorithm presented in Fig. 5.

The first (preliminary) field model was formulated in the FEMM 4.2 program using LUA script for: coil cross-sectional area 20 mm^2, number of turns 400, current value 3 A.

As simulation results obtained flux density distribution for both ducts of the throttle-return valve – see Fig. 6.

On the basis of simulation results determined (using the Bingham model) shear stress distribution of MR fluid – see Fig. 7.

The simulation results for the first model of the throttle-return valve showed that optimal properties of the MRF1040CG fluid could not be achieved (too low value of the magnetic flux

density), therefore the next simulations that were carried out aimed at selecting coil dimensions and supply parameters. The simulations for the diameter of the winding wire from 0.2 to 0.5 mm and for the maximum current value for each case were performed.

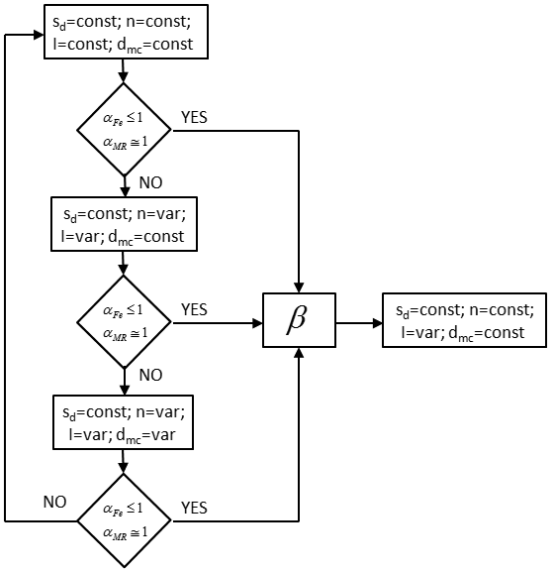

Fig. 5. Algorithm of the valve modelling process

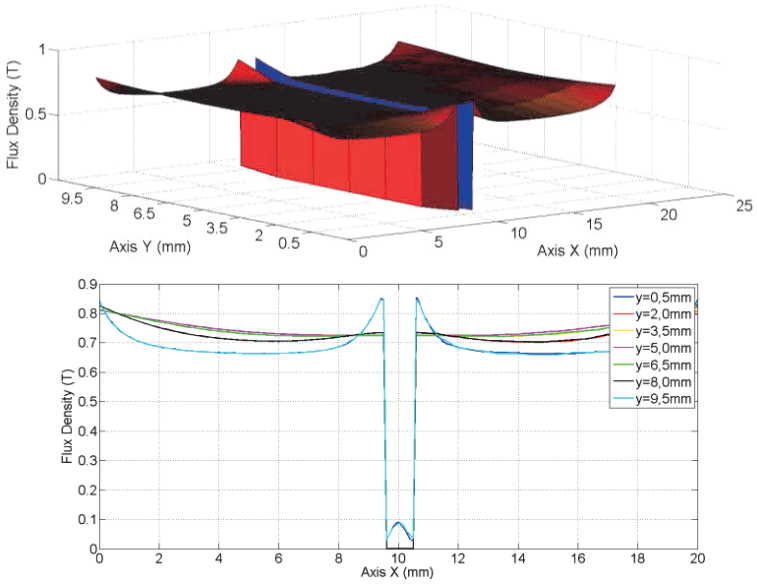

Fig. 6. Flux density distribution for both ducts of the throttle-return valve

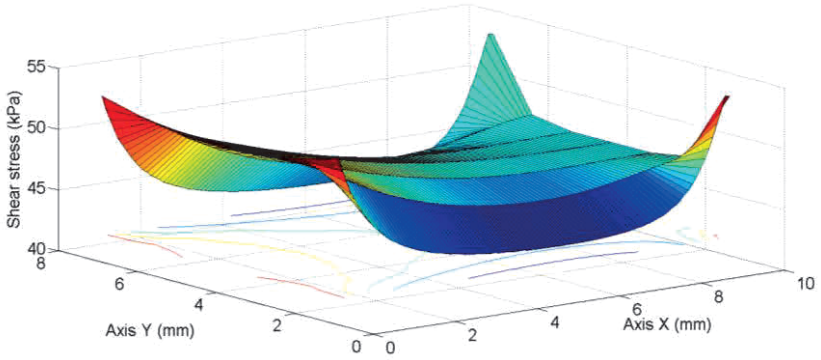

Fig. 7. Shear stress distribution for throttle duct of the throttle-return valve

In Table 1 the model parameters are presented together: current value, number of coils, wire diameter and simulation results: magnetic flux density for MR fluid and for magnetic core.

Table 1. Parameters and result for the simulation model

Sample number	Current value (A)	Number of coils (–)	Diameter of the wire (mm)	Magnetic flux density for fluid (B)	Magnetic flux density for magnetic core (B)
1	2.5	637	0.2	0.719	2.048
2	3.0	577	0.21	0.733	2.090
3	3.7	526	0.22	0.746	2.129
	...	...	...	...	...
29	83.4	111	0.48	0.947	2.762
30	90.5	106	0.49	0.953	2.786
31	98.2	102	0.5	0.961	2.816

Simulation results (magnetic flux density for MR fluid and magnetic core) from Table 1 in a graphical way are presented in Fig. 8.

The simulation results demonstrated that in order to achieve magnetic flux density for MR fluid about 1.1 T, without magnetic core saturation, it is necessary to change dimensions of the magnetic core.

The last simulation model was focused on selecting the value of magnetic core width and was performed for a magnetic core width from 5 to 7.5 mm (in increments of 0.5 mm) and for 31 cases presented in Table 1.

The value of magnetic flux density for MR fluid as well as for magnetic core, obtained by simulation, are presented in Fig. 9.

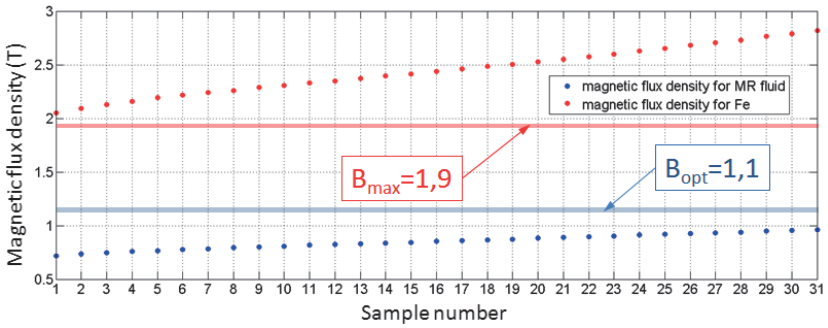

Fig. 8. Magnetic flux density for different 31 analyzed cases

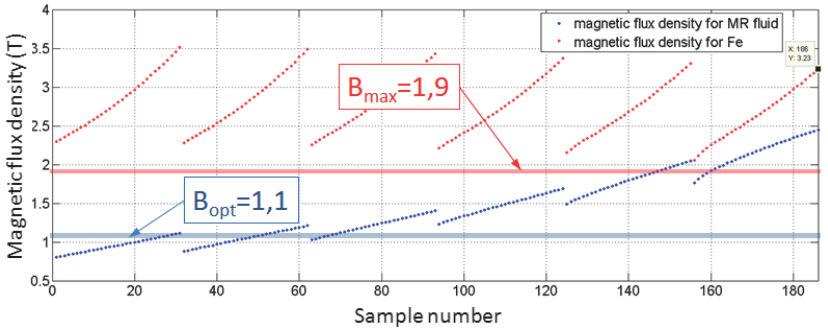

Fig. 9. Value of magnetic flux density for MR fluid and for magnetic core obtained for modified magnetic core

Obtained results of magnetic flux density were related to their maximum values:

$$\alpha_{Fe} = \frac{B_{Fe}}{B_{Fe\max}}, \quad \alpha_{MR} = \frac{B_{MR}}{B_{MR\max}}, \tag{3}$$

where: B_{Fe} is the magnetic flux density for magnetic core, $B_{Fe\max}$ is the maximum magnetic flux density for magnetic core, B_{MR} is the magnetic flux density for MR fluid, $B_{MR\max}$ is the maximum magnetic flux density for MR fluid,

The determined values of coefficient α_{Fe} and α_{MR} for analyzing 186 cases in a graphical way was shown in Fig. 10.

Next with the help of the coefficient β (4), the case was selected (number 94) for the last simulation model – see Fig. 11.

$$\beta = \beta_{\text{diff}} + abs(\beta_{sr}), \tag{4}$$

where:

$$\beta_{sr} = \frac{\alpha_{Fe} + \alpha_{MR}}{2}, \qquad \beta_{\text{diff}} = \alpha_{Fe} - \alpha_{MR}. \tag{5}$$

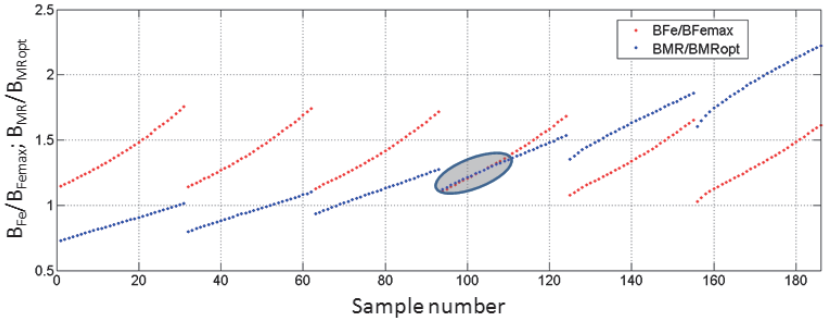

Fig. 10. Value of coefficient α_{Fe} and α_{MR}

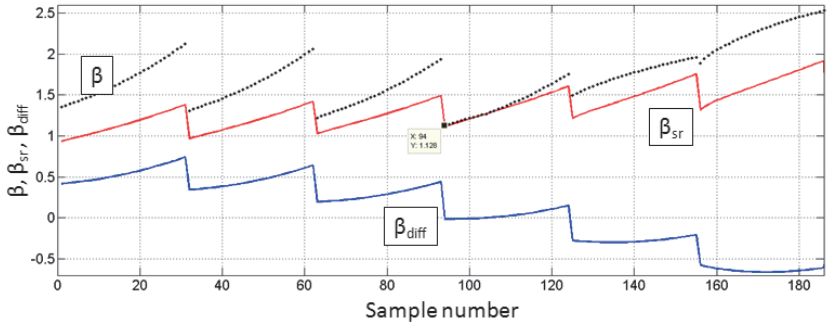

Fig. 11. Value of coefficient β, β_{diff} and β_{sr}

The last simulation model was performed for: the coil cross-sectional area equals 20 mm^2, the number of coils equals 637, the wire diameter equals 2.5 mm, the current value from 0.1 to 2.5 A (in increments of 0.1 A).

The curve of magnetic flux density for MR fluid as well as for magnetic core versus the current were obtained as the result of simulations – see Fig. 12.

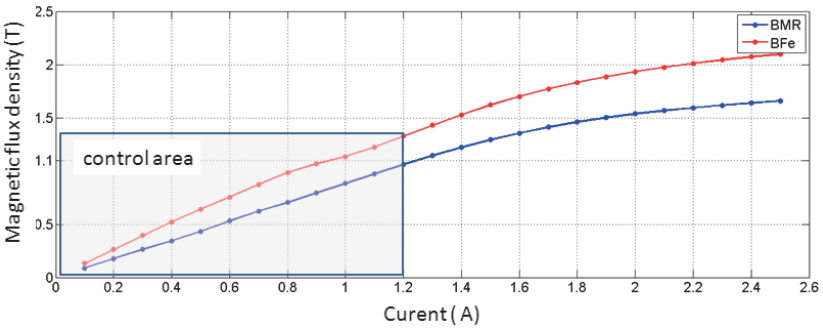

Fig. 12. Magnetic flux density for MR fluid and for magnetic core versus current curve

5. Maximum pressure value needed to close the valve

Next, an analysis was performed in order to determine the maximum pressure value of the MR fluid which is needed to close the valve ($Q_{\text{out}} = 0$). The analysis performed for one of the two ducts because both have the same dimensions and both can work as return or throttle valve.

The basic dimensions for the pressure analysis is shown in Fig. 13.

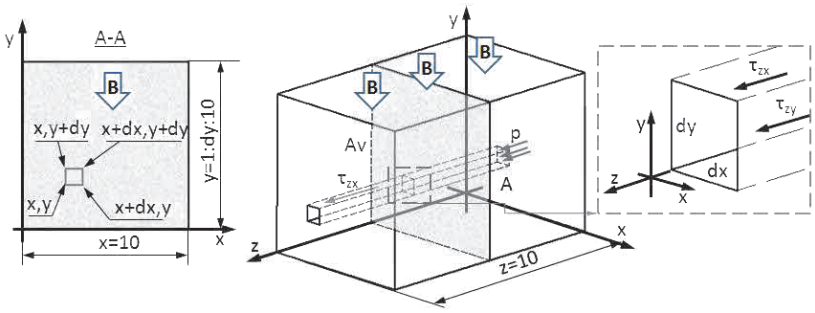

Fig. 13. Volume of the MR fluid with a separate infinitely small fluid volume z axis

The differential of the shear force is given by Equation (6):

$$dF = p \cdot dx \cdot dy, \tag{6}$$

where p is the the pressure acting on the infinitely small field $dS = dx \cdot dy$.

Shear stresses acting in the plane zx and zy are calculated by formula:

$$\tau_{zx} = \frac{dF}{dS_{zx}}, \qquad \tau_{zy} = \frac{dF}{dS_{zy}}, \tag{7}$$

where: $dS_{zx} = dx \cdot z$ is the area of impacts of the shear force dF for shear stress τ_{zx}, $dS_{zy} = dy \cdot z$ is the area of impacts of the shear force dF for shear stress τ_{zy},

The magnetic flux distribution in the cross-section marked A–A was determined – see Fig. 14.

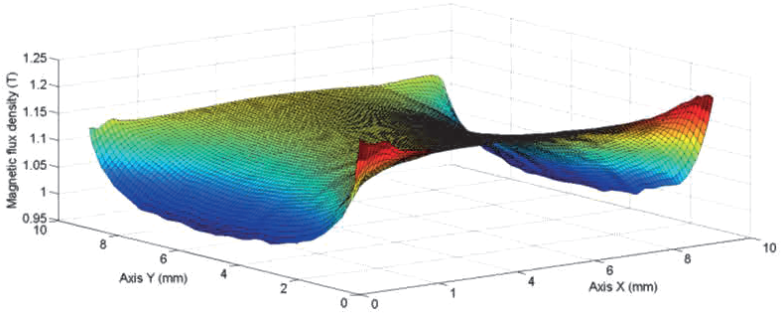

Fig. 14. Magnetic flux distribution in the cross-section A–A (Fig. 12)

The results shown in Fig. 14 were saved as matrix B_{xy} and next, using Equation (8) the matrix of the shear stress was determined (shown in graphical way in Fig. 15.).

$$[\tau_0] = -49.14 \cdot [B_{xy}]^3 + 62.4 \cdot [B_{xy}]^2 + 45.47 \cdot [B_{xy}] + 0.1959, \tag{8}$$

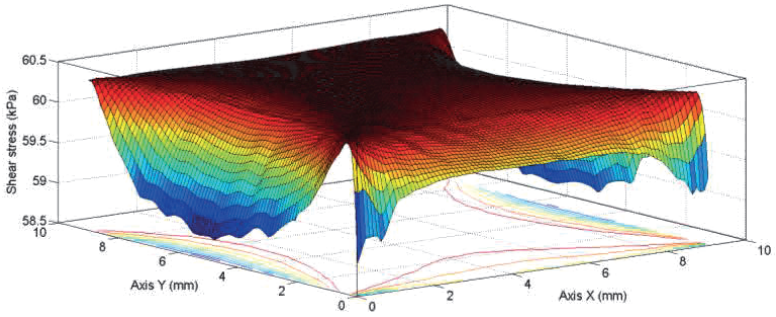

Fig. 15. Shear stress distribution in the cross-section A–A

Based on the distribution of shear stress in the cross-section and the dimensions of the duct the maximum pressure value was calculated with using Formulas (9), (10).

$$p_{zx} = \frac{\tau(B) \cdot z}{dy}, \qquad p_{zy} = \frac{\tau(B) \cdot z}{dx}, \tag{9}$$

$$p_{zx} = \frac{\tau(B) \cdot z}{y}, \qquad p_{zy} = \frac{\tau(B) \cdot z}{x}. \tag{10}$$

In paper [11] a formula is given of the maximum fluid pressure taking into account a component related to liquid viscosity Δp_η. The formula was transformed taking into account the size and axis mark in Fig. 13.

$$\Delta p = \Delta p_\eta + \Delta p_\tau = \frac{12 \cdot \mu \cdot Q_v \cdot z}{y^3 \cdot x} + \frac{c \cdot \tau(H) \cdot z}{y}, \tag{11}$$

where: dynamic viscosity μ Pa·s, orifice flow rate Q_v m^3/s, yield stress $\tau(H)$, z m, y m and x m represent respectively length, fluid gap and width of the flow orifice between the fixed magnetic poles (see Fig. 13), dimensionless constant c (varies between 2 and 3 [11]).

Next, the value of the pressure drop for which the valve works as an off-valve was determined. The calculation was performed for:

- variable value of y: $y = 1 : dy : 10$ (see Fig. 13),
- dynamic viscosity $\mu = 0.28$ Pa·s, fluid density MR $\rho = 3600$ kg/m^3, kinematic viscosity $\nu = \mu/\rho = 7.77\,\mathrm{e}^{-5}$ m^2/s,
- parameters of the actuator which cooperates with the valve: actuator speed $v_p = 0.1$ m/s, piston diameter $D_p = 0.1$ m, piston rod diameter $d_p = 0.03$ m, on this basis was calculated: area of the rod $A_p = \pi \cdot (D_p^2 - d_p^2)/4$ m^2 and flow rate $Q_p = A_p \cdot v_p$.

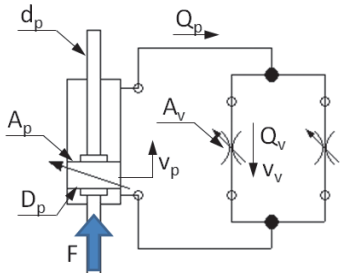

Fig. 16. Hydraulic schema: cylinder-valve

On the basis of the flow continuity principle $Q_p = Q_v$ (with known parameters A_p, v_p and A_v) the fluid flow speed was calculated:

$$v_v = \frac{Q_p}{A_v} = \frac{A_p \cdot v_p}{A_v}. \tag{12}$$

Using Equation (11), the values of the pressure drop as a function of the variable value of y were determined and are shown in Fig. 17.

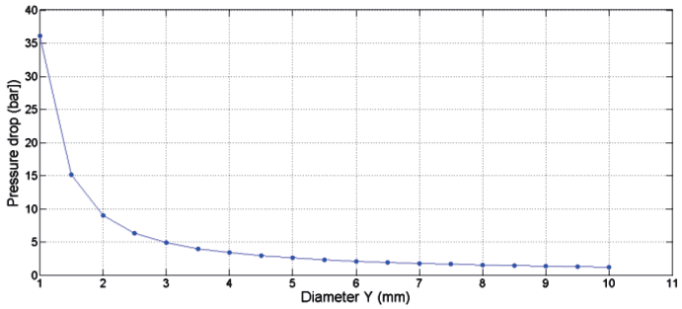

Fig. 2. Pressure drop (bar) vs. gap diameter y (mm)

Also, the Reynolds number for the fluid flow through the valve duct was calculated according to the equations:

$$R_e = \frac{v_v \cdot d_h}{\nu}, \qquad d_h = \frac{4A_v}{U}, \tag{13}$$

where: v_v m/s is the fluid flow speed into valve duct; dh m is the hydraulic diameter; ν m^2/s is the kinematic viscosity; duct area $A = x \cdot y$ m^2; constructional variable $U = 2 \cdot (x + y)$.

The value of the Reynolds number equals 918 for $y = 10$ mm and 1671 for $y = 1$ mm. The range of this value means that for flow rate Q_v (see Fig. 16) MR fluid flow will be laminar.

The maximum force F, which the system can transfer without displacement, determined as the product of the piston surface area and pressure value, equals 88 N for $y = 10$ mm and 2580 N for $y = 1$ mm.

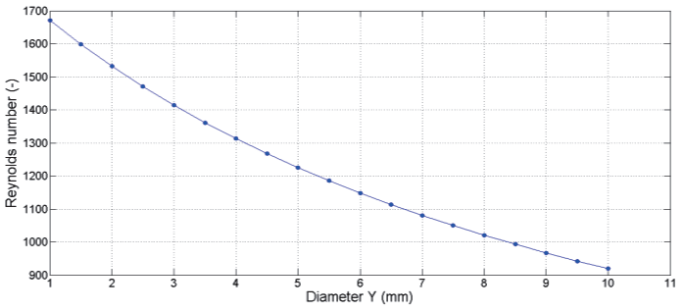

Fig. 3. Reynolds number (–) vs. gap diameter y (mm)

6. Conclusions

The paper presents the concept of the throttle-return valve intended for magnetorheological fluid.

For the proposed construction field calculation focused on coil parameters selection, power parameter selection and magnetic core dimension selection were performed. On the basis of Equations (3) to (5), the solution was selected for which, using Bingham model, shear stress distribution in the cross-section A–A was determined (Fig. 15).

The proposed construction, as opposed to the typical hydraulic solution, has no moving parts and allows one to regulate flow continuously in throttle and return part, and can work as a return valve, throttle valve, the off-valve or throttle-return valve. The proposed construction of the return-throttle valve for a magnetorheological fluid can be used for an advanced magnetorheological dumper.

Further works will include a return-throttle valve prototype with the use of 3D printing technology and optimization oriented on optimal selection of the: coil parameters, power parameters and magnetic core dimension.

References

[1] Abd Fatah A.Y., Mazlan S.A., Koga T., Zamzuri H., Zeinali M., Imaduddin F., *A review of design and modeling of magnetorheological valve*, International Journal of Modern Physics B, vol. 29, iss. 04 (2015), DOI: 10.1142/S0217979215300042.

[2] Kubík M., Mazůrek I., Roupec J., Strecker Z., Macháček O., *Design of Semi-active Magnetorheological Valve with Non-magnetic Bypass*, Transactions on Electrical Engineering, vol. 4, no. 1 pp. 20–23 (2015).

[3] Salloom M.Y., *Intelligent Magneto-Rheological Fluid Directional Control Valve*, International Journal of Innovation, Management and Technology, vol. 4, no. 4 (2013), DOI: 10.7763/ IJIMT.2013.V4.430.

[4] Salloom M.Y., Samad Z., *Finite element modeling and simulation of proposed design magneto-rheological valve*, Int. J. Adv. Manuf. Technol., pp. 421–429 (2011), DOI: 10.1007/s00170-010-2963-1.

[5] McLaughlin G., Hu W., Wereley N.M., *Advanced magnetorheological damper with a spiral channel bypass valve*, Journal of Applied Physics 115, 17B532 (2014), DOI: 10.1063/1.4869278.

[6] Szeląg W., *Electromagnetic converters with magnetorheological fluid* (in Polish), Publishing House of Poznan University of Technology, Poznań (2010).

[7] Szeląg W., Sujka P., Walendowski R., *Analysis of coupled phenomena in magnetorheological fluid devices*, XIV International Symposium Micromachines & Servodrives MiS'04, Tuczno, pp. 155–162 (2004).

[8] Wang D.H., Ai H.X., Liao W.H., *A magnetorheological valve with both annular and radial fluid flow resistance gaps*, Smart materials and structures, vol. 8, no. 11, pp. 269–273 (2009), DOI: 10.1088/0964-1726/18/11/115001

[9] Yokota S., Yoshida K., Kondoh Y., *A pressure control valve using MR fluid*, Proc. Forth JHPS-ISFP Tokyo 99, pp. 377–380 (1999).

[10] Yoshida K., Takahashi H., Yokota S. et al., *A bellows-driven motion control system using a magneto-rheological fluid*, Proceedings of the JFPS International Symposium on Fluid Power, vol. 2002, pp. 403–408 (2002).

[11] Sulakhe V.N., Thakare C.Y., Aute P.V., *Review – MR Fluid and Its Application*, International Journal of Research in Aeronautical and Mechanical Engineering, vol. 1, iss. 7, pp. 125–133 (2013).

[12] www.rheonetic.com, LORD Corporation.